Review of the LPM local positioning measurement system

Conference Paper · June 2012

DOI: 10.1109/ICL-GNSS.2012.6253104

4 authors, including:

Andreas Resch
Fachhochschule Oberösterreich
1 PUBLICATION **10** CITATIONS

SEE PROFILE

Review of the LPM Local Positioning Measurement System

Andreas Resch
Inmotiotec GmbH,
Abatec Group,
Oberregauer Str. 48
4844 Regau, Austria
Email:
a.resch@inmotiotec.com

Reimar Pfeil
Linz Center
of Mechatronics (LCM)
GmbH,
Altenbergerstr. 69
4040 Linz, Austria
Email:
reimar.pfeil@lcm.at

Marco Wegener
Institute for
Traffic Safety
and Automation
Engineering,
TU Braunschweig
38106 Braunschweig, Germany
Email:
wegener@iva.ing.tu-bs.de

Andreas Stelzer
Institute of
Communications Engineering
and RF-Systems,
Johannes Kepler
University (JKU) Linz
4040 Linz, Austria
Email:
a.stelzer@nthfs.jku.at

***Abstract*—Precise and accurate position estimation has become crucial to solving many technical problems. This contribution gives an overview of the LPM local positioning measurement system, which is based on the frequency-modulated continuous-wave radar principle. LPM uses two active transponders within each measurement cycle: one acts as a time reference for all base stations, while the other is mounted on the object whose position is to be determined. By evaluating the time-difference of arrival at several base stations surrounding the measurement field, the position can be precisely estimated. We demonstrate this using measurement data.**

***Index Terms*—LPM, local positioning, GNSS verification.**

I. Introduction

In the keynote speech of the 13th IAIN[1] world congress, David Last from the University of Wales, UK, outlined the development of navigation and positioning in the past two decades. Without doubt, the greatest accomplishment in this area was the satellite-based Global Positioning System (GPS), which provides worldwide positioning services to both the military and the public [1]. Since GPS has become the reference system for navigation, present and future global navigation satellite-based systems (GNSS) such as GLONASS [2] and Galileo [3] must provide backward compatibility with GPS. However, Last also criticized the inevitable dependence on GPS, which means higher susceptibility to jamming and disturbance. Furthermore, GPS has limits which may conflict with actual applications:

- no positioning in an indoor environment
- low measurement rate (1 Hz)
- coarse accuracy and precision in certain areas (e.g., urban, industrial, mountains).

These disadvantages led to the development of local positioning systems intended to bridge the gap between ultra-precise (e.g., laser-based) and long-range positioning. Numerous systems that provide a wide range of achievable accuracy and precision are currently commercially available. A short overview of the currently most widely used systems is given in Table I. Note that some systems are still under development, and detailed information can therefore not be provided in some cases.

This paper focuses on the LPM local positioning system, which was first presented in [4]. Since it supports real-time measurements with an update rate of 1000 Hz and a precision of several centimeters standard deviation for static measurements, the LPM system has not only proved itself in the market place for motion tracking applications (e.g., sports activities, tracking of vehicles and flying objects), but is also capable of providing a reference for other long-range positioning systems. A short description of the LPM system is given in the next section.

II. The LPM measurement system

A. Mode of operation

The LPM system is based on the bi-static frequency-modulated continuous-wave (FMCW) radar principle [12], realized in the 5.8 GHz ISM band with a bandwidth of 150 MHz and a ramp duration of about 500 µs. In a basic LPM system setup, several base stations (BSs) surround the measurement field, and a reference transponder (RT) is placed near the center of the field. The positions of the BSs and the RT are known. In the initialization phase, a single BS, the master BS, triggers the RT, which emits periodically a chirp to provide a common time base. After all BSs have been synchronized, the master BS activates the measurement transponder (MT), the position of which is to be estimated. MT and RT hardware are identical, and thus the only difference between these two transponders (TPs) is the mode of operation: the RT transmits its chirp autonomously and periodically, while the MT waits for a new activation command after each activation. In a multi-MT scenario, activation of the MTs switches from one to the next with each measurement cycle. This time division multiple access (TDMA) scheme guarantees that multiple MTs do not interfere with each other. Data from all BSs are collected by a data transfer network and passed to a master processing

[1]International Association of Institutes of Navigation

Table I
OVERVIEW OF CURRENTLY AVAILABLE LOCAL POSITIONING SYSTEMS.

Name	Measurement principle	Bandwidth in MHz	Accuracy[1] in cm	Update rate in Hz	Maximum range in m
LPR (Symeo) [5], [6]	FMCW	150	6-20	1000	several 100
Nanotron [7], [8]	CSS[2]	80	40-100	N/A[4]	900
Ubisense [9], [10]	UWB[3]	2000	13-23	33.75	N/A[4]
Decawave [11]	UWB	500	10-90	N/A[4]	N/A[4]
LPM (Abatec Group)	FMCW	150	2-50	1000	1500

[1] based on measurement data
[2] chirp spread spectrum (CSS)
[3] ultra-wideband (UWB)
[4] information not available

unit (MPU), where the position estimation is computed. A summary of the LPM principle is shown in Fig. 1.

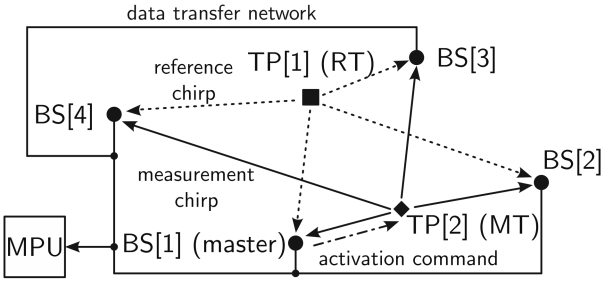

Figure 1. LPM mode of operation with 4 BSs surrounding the field of view. The Master BS activates RT and MT via an activation command. The chirps emitted from the RT and MT are collected and evaluated by all BSs separately and sent to the MPU via a data transfer network.

B. Pseudo-range generation

In general, the time-of-flight (TOF) between the BS and TP is in the nano- to microseconds range, and thus evaluation in the frequency domain is chosen. Within one measurement cycle, the rth BS, where $r = 1, 2, \dots R$ and R denotes the total number of BSs, receives the signals from the RT and the MT and evaluates the time difference of arrival (TDOA) by estimating their IF frequencies. Hence, the estimated TDOA is given as

$$\hat{t}_{\mathrm{TDOA},r} = \frac{1}{k}\left(\hat{f}_2 - \hat{f}_1\right) \tag{1}$$

with $k = B/T$ denoting the chirp rate composed of the bandwidth B and the duration of the ramp T. In (1), $\hat{f}_2$ and $\hat{f}_1$ are the estimated frequencies of the signal from the MT and the RT respectively. Estimation of the frequencies requires a power spectrum estimation, which is generally performed by using the Schuster periodogram [13, Ch. 14]. An overview of the derivation of $\hat{t}_{\mathrm{TDOA},r}$ is given in Fig. 2. The pseudo-range for the rth BS then follows from (1):

$$\hat{\rho}_r = c_0 \hat{t}_{\mathrm{TDOA},r}, \tag{2}$$

where c_0 is the propagation velocity of the electromagnetic wave in air.

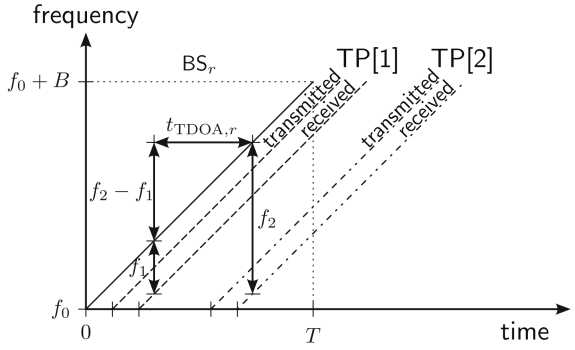

Figure 2. Signal map of an arbitrary BS_r to explain the derivation of (1). f_0 denotes the start frequency of the chirp.

C. Hardware components

As previously mentioned, the LPM generally consists of two main hardware components: The BS and the TP, the latter either in reference or in measurement mode.

1) The BS: A block diagram of the BS in reception mode is given in Fig. 3. The entire process is coordinated by the field-programmable gate array (FPGA) in the upper left corner. At the beginning of the receiving phase, the FPGA instructs the direct digital synthesizer (DDS) to generate a chirp signal, which is converted to 5.8 GHz by the phase-locked loop (PLL) and the voltage controlled oscillator (VCO). The subsequential switches redirect the chirp to the local oscillator (LO) port of the mixer, and thus the signal received from the antenna amplified by the low noise amplifier (LNA) is mixed with the chirp. The intermediate frequency (IF) must pass a bandpass filter, which reduces the direct current (DC) level and ensures the sampling theorem $f < 2f_\mathrm{s}$ with f_s denoting the sampling frequency. Finally, the IF signal is digitized by an analogue to digital converter (ADC) and evaluated by a digital signal processor (DSP). The frequency estimation is performed by the DSP as described above. In transmission mode (alternative position of switches), the master BS generates the activation

command, which is amplified by the power amplifier (PA). A photo of the BS printed circuit board (PCB) is given in Fig. 4.

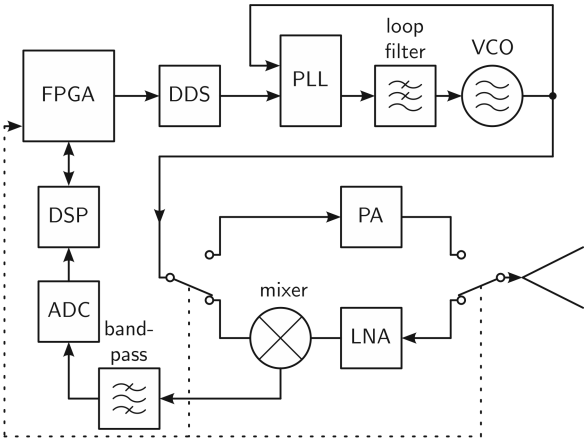

Figure 3. Block diagram of the BS (in reception mode) of an LPM system.

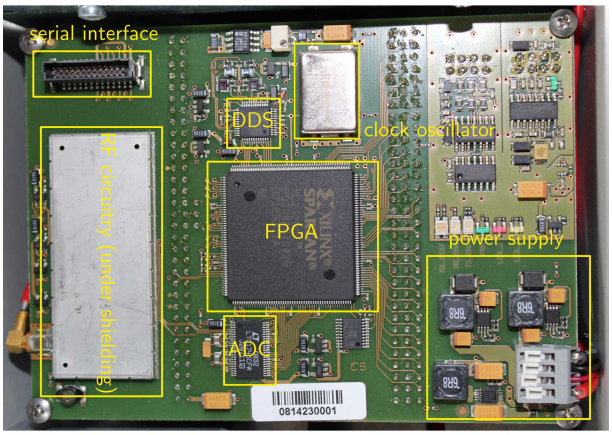

Figure 4. Photograph of the BS PCB.

2) The TP: The basic layout of the TP, depicted in Fig. 5, is very similar to that of the BS, but all hardware components are optimized for low power consumption. The main difference is that the TP incorporates a frequency shift keying (FSK) decoding chip, which determines whether the TP activation command is within the received signal. If this is the case, the MT switches automatically to transmission mode and transmits the chirp signal together with the optional telemetry information. A photo of the TP PCB is given in Fig. 6.

3) Backbone network: As shown in Fig. 1, the LPM system also requires a data network for synchronous transfer of the evaluated pseudo-ranges from the BSs to the MPU. For this purpose, two system versions are sold by Abatec: the premium version uses a fiber optic network, which ensures maximum shielding against interference signals, while the LPM light version uses a wireless local area network (WLAN), which requires no expansive wiring. However, the latter has the drawback of being more easily disrupted by interference and

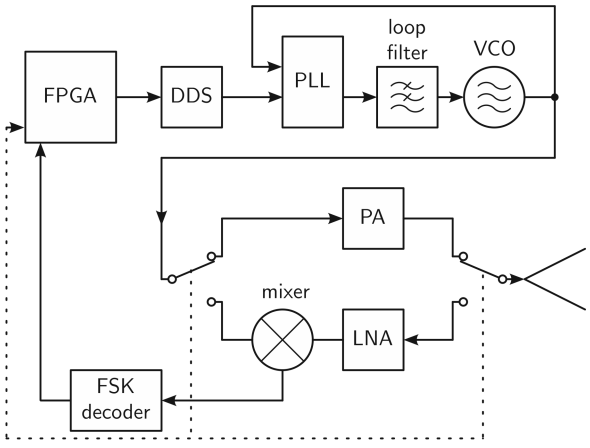

Figure 5. Block diagram of the TP in transmission mode.

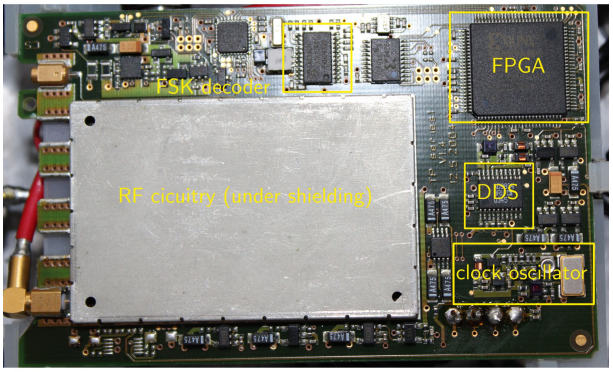

Figure 6. Photograph of the TP PCB.

requires transmission of the TP identification number through the telemetry channel.

D. Position estimation

Estimating the position requires the parameter vector

$$\boldsymbol{\Theta}_{\mathrm{p}} = \left[\begin{array}{cc} \mathbf{c}_{\mathrm{MT}}^{\mathrm{T}} & r_{\mathrm{MT}} \end{array} \right]^{\mathrm{T}} \tag{3}$$

to be estimated, where $\mathbf{c}_{\mathrm{MT}} = \left[\begin{array}{ccc} x_{\mathrm{MT}} & y_{\mathrm{MT}} & z_{\mathrm{MT}} \end{array} \right]^{\mathrm{T}}$ are the Cartesian coordinates of the MT, and r_{MT} is a range offset which originates from the unknown activation time of the MT. The function which links the measured pseudo-ranges of (2) to (3) is given by

$$\rho[r] = \|\mathbf{c}_{\mathrm{BS},r} - \mathbf{c}_{\mathrm{MT}}\| - \|\mathbf{c}_{\mathrm{BS},r} - \mathbf{c}_{\mathrm{RT}}\| + r_{\mathrm{MT}} \tag{4}$$

with $\mathbf{c}_{\mathrm{BS},r}$, $\mathbf{c}_{\mathrm{RT}}$ as the Cartesian coordinates of the rth BS and of the RT respectively, and $\|\ldots\|$ denotes the Euclidean norm function. By using the transformation $\rho'[r] = \rho[r] + \|\mathbf{c}_{\mathrm{BS},r} - \mathbf{c}_{\mathrm{RT}}\|$, we can rewrite (4) as

$$\rho'[r] = \|\mathbf{c}_{\mathrm{BS},r} - \mathbf{c}_{\mathrm{MT}}\| + r_{\mathrm{MT}}, \tag{5}$$

which is identical to the GPS equation, and thus all GPS positioning algorithms can easily be applied to LPM [14].

1) Robust position estimation: As in the GPS system, false measurements due to multipath signals must be considered. Note that LPM can evaluate only the line-of-sight (LOS) paths between the TP and the BS, and considers all non-line-of-sight (NLOS) signals defective. The following methods can be used to mitigate the influence of NLOS signals on the LPM system:

- Using an alternative solver: In [15], a position estimator based on the least median square (LMS) was derived. However, it is less efficient than, for instance, the Bancroft algorithm [16] and requires significantly higher computational effort.
- Monitoring the pseudo-ranges for outliers: By taking advantage of the inherent drift of the pseudo-ranges, a Kalman filter which checks the temporal consistency of the pseudo-ranges was derived [17].
- Joint power level and pseudo-range positioning: As presented in [18], the power level of each TP is a direct measurement value for the LOS and can thus be used to identify corrupted BSs.

III. Measurement Results

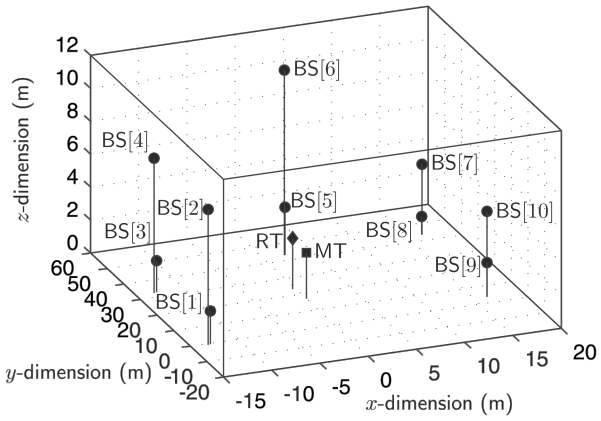

(a)

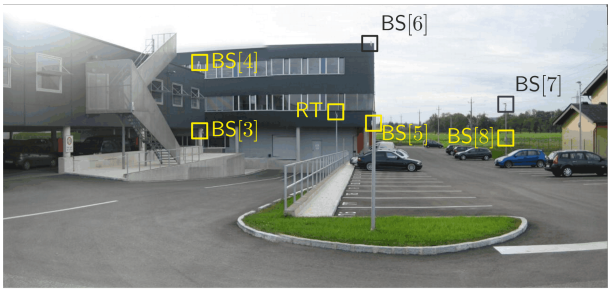

(b)

Figure 7. (a) Top view of schematic diagram of the LPM setup at the test site and (b) photograph taken at approximately position $x = 0$ m, $y = -20$ m looking in the direction of BS[5]. The true position of the RT is $x = -0.327$ m, $y = 23.575$ m, $z = 1.588$ m and of the MT $x = -0.002$ m, $y = 17.068$ m, $z = 1.297$ m.

In this section, an exemplary LPM measurement result is presented. The measurements were performed at the LPM test site in Regau, Austria. Fig. 7 shows a schematic overview and a photograph of the measurement site. Fig. 8 illustrates the differences between estimated and true positions of the MT in the x, y and z dimensions. The true position of the MT was determined using a Trimble 3305 tachymeter with a measurement accuracy of $\pm(3\,\text{mm}+2\,\text{ppm})$ in direct reflex mode. Based on the measurement results, the standard deviation of the d-dimension is evaluated by

$$\sigma_d = \left(\frac{1}{N-1} \sum_{n=1}^{N} \left(\hat{d}(n) - \overline{d} \right)^2 \right)^{\frac{1}{2}}, \tag{6}$$

where $\hat{d}(n)$ is the estimated dimension for the nth measurement cycle with its mean value $\overline{d} = \frac{1}{N} \sum_{n=1}^{N} \hat{d}\,(n)$ and the total number of measurement cycles N. Moreover, the bias can be estimated by

$$\Delta d = \overline{d} - d_{\text{true}} \tag{7}$$

with d_{true} as the true value for the dth dimension. The standard deviations and the bias of the measurements are summarized in Table II.

By means of the geometric dilution of precision (GDOP) concept [19], general 3D position estimation with the given setup is possible. However, the BSs are positioned only at three different levels in the z-direction, and thus increased variance as shown in Fig. 10 is inevitable. Nevertheless, the results shown in Figs. 8, 9, and 10 corroborate the system performance stated in Table I.

Table II
Standard deviation of static LPM measurements with $N = 1 \cdot 10^5$.

Dimension	(7) in mm	(6) in mm
x	-16.19	31.86
y	-7.03	16.56
z	-77.65	99.99

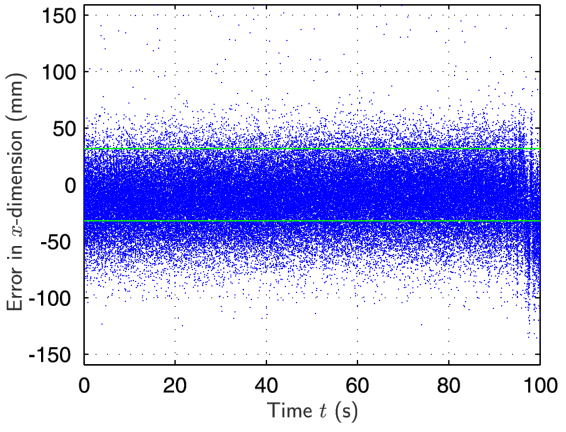

Figure 8. x-dimension position estimation errors of the LPM system at the test site shown in Fig. 7. The green lines mark the $\pm\sigma_x$ bound.

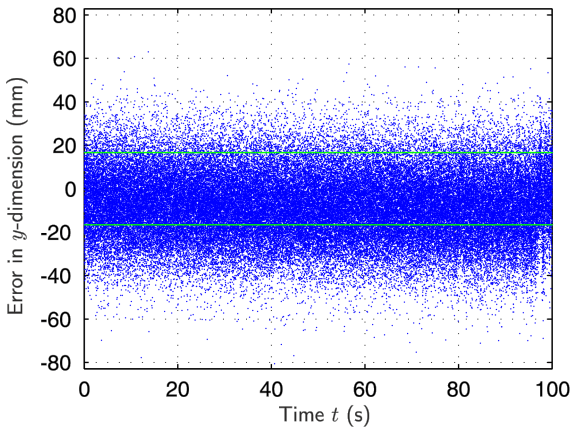

Figure 9. y-dimension position estimation errors of the LPM system at the test site shown in Fig. 7. The green lines mark the $\pm\sigma_y$ bound.

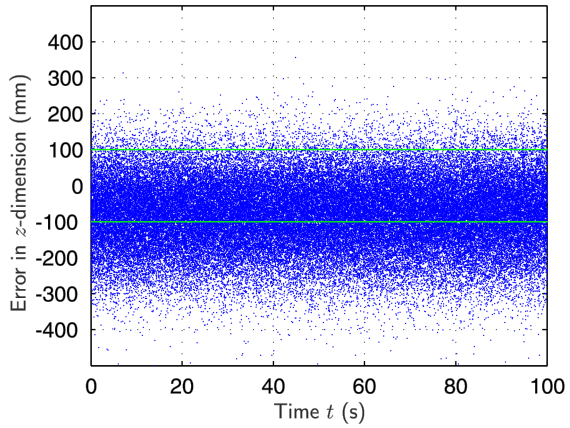

Figure 10. z-dimension position estimation errors in of the LPM system at the test site shown in Fig. 7. The green lines mark the $\pm\sigma_z$ bound.

IV. Conclusions

We have presented the LPM measurement system as a reliable tool for local position estimation. We have described the general measurement principle and analyzed the performance of the LPM system in static measurements. The results of the static experiments show that the LPM system is a highly precise and accurate positioning tool. The precision can be improved even further by using an (extended) Kalman filter [20]. The LPM system will be used in the FP7 project QualiSaR as reference localization system for determining the GNSS accuracy performance in the field of road traffic applications.

Acknowledgment

This work was funded by the COMET K2 Center "Austrian Center of Competence in Mechatronics (ACCM)" and the QualiSaR project of the European GNSS Agency (GSA). The comet program is funded by the Austrian federal government, the federal state Upper Austria, and the scientific partners of ACCM. The authors would like to thank Philipp Jöchl, Lukas Redlinger and Bernhard Leithenmair from Abatec Group AG for their support in conducting the LPM measurements.

References

[1] E. D. Kaplan and C. J. Hegarty, *Understanding GPS - Principles and Applications*, Artech House, Norwood, 2nd edition, 2006.

[2] "Information-Analytical centre of coordinate-time and navigation support," http://www.glonass-center.ru/en/, Feb. 2012.

[3] "The Galileo System," http://www.gsa.europa.eu/, Feb. 2012, [Online].

[4] A. Stelzer, K. Pourvoyeur, and A. Fischer, "Concept and Application of LPM - A Novel 3-D Local Position Measurement System," *IEEE Transactions on Microwave Theory and Techniques (MTT)*, vol. 52, pp. 2664–2669, Dec. 2004.

[5] M. Vossiek, L. Wiebking, P. Gulden, J. Weighardt, and C. Hoffmann, "Wireless local positioning - concepts,solutions,applications," in *Proceedings of the Radio and Wireless Conference (RAWCON)*, Aug. 2003, pp. 219–224.

[6] L. Wiebking, M. Glänzer, D. Mastela, M. Christmann, and M. Vossiek, "Remote Local Positioning Radar," in *Proceedings of the Radio and Wireless Conference (RAWCON)*, Sep. 2004, pp. 191–194.

[7] "Real Time Location System (RTLS) - White Paper," http://www.nanotron.com/EN/pdf/WP_RTLS.pdf, Feb. 2012, [Online].

[8] C. Röhrig and Sarah Spieker, "Tracking of Transport Vehicles for Warehouse Management using a Wireless Sensor Network," in *Proceedings of the IEEE/RSJ International Conference on Intelligent Robots and Systems*, Sep. 2008.

[9] "Ubisense RTLS solutions," http://www.ubisense.net/en/, Feb. 2012, [Online].

[10] A. Prorok, A. Arfire, A. Bahr, J. R. Fraserotu, and A. Martinoli, "Indoor Navigation Research with the Khepera III Mobile Robot: An Experimental Baseline with a Case-Study on Ultra-Wideband Positioning," in *Proceedings of the International Conference on Indoor Positioning and Indoor Navigation (IPIN)*, Sep. 2010.

[11] Tingcong Ye, M. Walsh, P. Haigh, J. Barton, A. Mathewson, and B. O'Flynn, "Experimental Impulse Radio IEEE 802.15.4a UWB Based Wireless Sensor Localization Technology: Characterization, Reliability and Ranging," Tech. Rep., Tyndall National Institute, University College Ireland, UCC, Cork, Jun. 2011.

[12] A.G. Stove, *Linear FMCW Radar Techniques*, vol. 139(5), pp. 343–350, IEEE Proc. Radar Signal Processing, 1992.

[13] J. G. Proakis and D. G. Manolakis, *Digital Signal Processing - Principles, Algorithms and Applications*, Prentice Hall PTR, Upper Saddle River, NJ, 4th. edition, 2007.

[14] K. Pourvoyeur, A. Stelzer, and G. Gassenbauer, "Position Estimation Techniques for the Local Position Measurement System LPM," in *Proceedings Asia Pacific Microwave Conference (APMC) on CD-ROM*, Dec. 2006, pp. 1509–1514.

[15] R. Pfeil, S. Schuster, P. Scherz, A. Stelzer, and G. Stelzhammer, "A Robust Position Estimation Algorithm for a Local Positioning Measurement System," in *Proceedings of the International Microwave Workshop Series on Wireless Sensing, Local Positioning and RFID (IMWS)*, Sep. 2009.

[16] S. Bancroft, "An Algebraic Solution of the GPS Equations," *IEEE Transactions on Aerospace and Electronic Systems (AES)*, vol. 21(7), pp. 56–59, Jan. 1985.

[17] R. Pfeil, K. Pourvoyeur, A. Stelzer, and G. Stelzhammer, "Distributed Fault Detection for Precise and Robust Local Positioning," in *Proceedings of the 13th IAIN World Congress and Exhibition*, 2009.

[18] R. Pfeil, M. Pichler, P. Scherz, A. Stelzer, and G. Stelzhammer, "Power-Level Surveillance for an FMCW-based Local Positioning System," in *Proceedings of the International Conference on Indoor Positioning and Indoor Navigation (IPIN)*, Sep. 2010.

[19] J. Zhu, "Calculation of geometric dilution of precision," *IEEE Transactions on Aerospace and Electronic Systems*, vol. 28, no. 3, pp. 893–895, Jul. 1992.

[20] K. Pourvoyeur, *Position Estimation, Tracking, and Sensor Fusion of the Local Position Measurement System LPM*, Ph.D. thesis, Johannes Kepler University, Linz, Austria, Nov. 2007.